

September 5, 2022

A fast matrix-free algorithm for spectral approximations to the Schrödinger equation

Bernd Brumm

Mathematisches Institut, Universität Tübingen, Auf der Morgenstelle 10, D-72076 Germany.¹

Abstract. We consider the linear time-dependent Schrödinger equation with a time-dependent smooth potential on an unbounded domain. A Galerkin spectral method with a tensor-product Hermite basis is used as a discretization in space. Discretizing the resulting ODE for the Hermite expansion coefficients involves the computation of the action of the Galerkin matrix on a vector in each time step. We propose a fast algorithm for the direct computation of this matrix-vector product without actually assembling the matrix itself. Together with the application of a hyperbolically reduced basis, this reduces the computational effort considerably and helps cope with the infamous curse of dimensionality. The error analysis is based on a representation of the three-term recurrence relation for the one-dimensional Hermite functions as a binary tree. The fast algorithm constitutes an efficient tool for schemes involving the action of a matrix due to spectral discretization on a vector, to be applied also in the context of spectral approximations for linear problems other than the Schrödinger equation. **Keywords:** linear Schrödinger equation, spectral Galerkin methods, reduced index sets, fast algorithm, direct computation, curse of dimensionality, binary trees

Introduction

We consider the linear time-dependent Schrödinger equation

$$i \frac{\partial}{\partial t} \psi(x, t) = (H\psi)(x, t) = -\frac{1}{2}(\Delta\psi)(x, t) + V(x, t)\psi(x, t), \quad x = (x_1, \dots, x_N) \in \mathbb{R}^N \quad (1)$$

in N spatial dimensions with a possibly time-dependent multiplicative potential V that meets certain regularity conditions on a cube $\Omega = [-L, L]^N$ and a solution $\psi(\cdot, t)$ that is essentially supported within Ω , for all times $t \in [0, T]$. For an underlying geometry as simple as in (1), spectral methods are a natural means of discretization in space. In a naive approach, the resulting ODE system grows exponentially in N , making an accurate approximation practically unfeasible even for moderate choices of N . For this difficulty, the catch phrase *curse of dimensionality* has been coined. Time propagation typically requires computing the action of the Galerkin matrix on a vector in each step, and, in case of a time-dependent potential, the matrix has to be re-assembled.

A promising strategy is a suitable reduction of the spectral approximation basis. E.g.,

¹E-mail:brumm@na.uni-tuebingen.de.

[15, 16] study a spectral approach with collocation on a sparse grid in case of a time-independent potential and periodic boundary conditions with a hyperbolically reduced tensor-product Fourier basis. [19], Chapter III.1.4, points out that, unlike on a full grid, the resulting coefficient ODE does not exhibit a Hermitian matrix, which possibly gives rise to numerical troubles and limits the range of applicable time-stepping methods. As a remedy, a Fourier Galerkin method in combination with an approximation of the potential by a trigonometric polynomial is proposed. We adopt this basic idea from the simpler setting of a periodic problem.

In the present paper, we also employ a spectral Galerkin approach with a reduced basis in combination with a polynomial approximation of (parts of) the potential, but we consider an unbounded domain instead of a periodic problem. Hermite functions are a natural and, thus, widely-used spectral basis for the Schrödinger equation on unbounded domains, see, e.g., [19], Chapter III.1, [11] for the linear and [13] for a nonlinear case. Furthermore, we allow the potential to be time-dependent.

Besides basis reduction and potential approximation, we develop a fast algorithm for the direct (i.e., matrix-free) computation of the aforementioned matrix-vector-product that further speeds up propagation in time considerably. The basic idea for the fast algorithm was proposed in [12] in the context of a splitting procedure for the linear Schrödinger equation in the semi-classical regime: We use a recurrence relation for the univariate Hermite functions and orthogonality to define (never actually assembled) coordinate matrices for each coordinate direction that act directly on vectors. These matrices are then formally inserted into the polynomially approximated potential. In the present paper, it is shown that this is equivalent to a suitable entrywise approximation of the Galerkin matrix by Gauss-Hermite quadrature, which is derived as is commonly done in the context of Discrete Variable Representations, see [18]. However, this is only true if the matrices are indexed over a full set of multi-indices. We give a detailed analysis for the resulting quadrature error as well as for the error due to a hyperbolical index reduction based on binary tree representations. Both errors are well-behaved if the potential can be sufficiently well approximated by a multivariate polynomial. If so, we get bounds $C(\mathcal{R}, W)K^{-\beta}$ and $C(N, \mathcal{R}, W, \beta, L)K^{-\beta}$ for the errors due to quadrature and grid reduction, respectively. Here, W is the part of the potential V that is approximated over an N -dimensional index set $\mathcal{R}(R)$ with maximal univariate polynomial degree R , $K \gg R$ is the maximal number of basis functions employed in each coordinate direction in the Galerkin approximation, and the coefficients of the approximate solution exhibit a decay of order β with increasing index. The fast algorithm scales essentially linearly in K .

We avoid quadrature at all. In contrast, in the chemical literature, there is a matrix-free approach based on ingenious sequential summations for the matrix-vector product that employs a (still exponentially large) reduced basis and treats the problem of huge quadrature-grids using a nonproduct Smolyak grid quadrature, see [2, 3, 4, 5, 6]. We are not aware of any further matrix-free approaches to treat the action of this Galerkin matrix on a vector efficiently.

The fast algorithm constitutes a useful tool for a variety of time integration schemes. The strategy is generic, hence, it is serviceable also for spectral Galerkin approximations to other linear problems where a Galerkin basis of algebraic orthogonal polyno-

mials is involved.

In Section 1, we deduce the ODE system for the Hermite expansion coefficients from the Galerkin ansatz with a reduced index set and a polynomially approximated potential. Section 2 briefly outlines the discretization in time by Magnus integrators, where the matrix exponential is approximated using the Lanczos method. In Section 3, we present the fast algorithm for the matrix-free computation of the action of the Galerkin matrix on a vector in each Lanczos step and illustrate the computational speed-up. The connection between the fast algorithm and Gauss-Hermite quadrature for the Galerkin matrix is shown in Section 4. A detailed error analysis is given in Section 5. Section 6 presents some numerical experiments confirming the theoretical results.

1 Semi-discretization in space

1.1 Hermite basis

Starting from $\varphi_{-1} \equiv 0$ and $\varphi_0(x) = \pi^{-1/4} e^{-x^2/2}$, the three-term recurrence relation ($k \geq 0$)

$$x\varphi_k(x) = \sqrt{\frac{k+1}{2}}\varphi_{k+1}(x) + \sqrt{\frac{k}{2}}\varphi_{k-1}(x), \quad (2)$$

yields a complete $L^2(\mathbb{R})$ -orthonormal set $\{\varphi_k\}_{k \in \mathbb{N}}$ of Schwartz functions, in particular, $(\varphi_j, \varphi_k) = \delta_{jk}$, where $(f, g) = \int f\bar{g}$ denotes the standard L^2 -inner product. An explicit expression is $\varphi_k(x) = \pi^{-1/4} (2^k k!)^{-1/2} H_k(x) e^{-x^2/2}$, where H_k denotes the classical Hermite polynomial of degree k . The Hermite functions are readily seen to be the eigenfunctions of the harmonic oscillator, i.e.,

$$\frac{1}{2}(p^2 + q^2)\varphi_k = \left(k + \frac{1}{2}\right)\varphi_k, \quad (3)$$

where $(q\psi)(x) = x\psi(x)$ and $(p\psi)(x) = -i\frac{\partial}{\partial x}\psi(x)$ denote the position and momentum operators, respectively, see, e.g., [1], Section 22, [19], Chapter III.1.1, or [22], Section 7.7, for the construction of the Hermite basis and useful facts. In higher dimensions, we consider tensor-products of Hermite functions, i.e.,

$$\varphi_{\mathbf{k}}(x) = \varphi_{k_1}(x_1) \cdots \varphi_{k_N}(x_N),$$

where $\mathbf{k} = (k_1, \dots, k_N) \in \mathbb{N}^N$ is a multi-index and φ_{k_l} are univariate Hermite functions as above, $1 \leq l \leq N$. Again, $\{\varphi_{\mathbf{k}}\}_{\mathbf{k} \in \mathbb{N}^N}$ is a complete $L^2(\mathbb{R}^N)$ -orthonormal set of functions. Due to the eigenfunction property (3), we find

$$\frac{1}{2} \sum_{l=1}^N (p_l^2 + q_l^2) \varphi_{\mathbf{k}} = \frac{1}{2} \left(-\Delta + \sum_{l=1}^N q_l^2 \right) \varphi_{\mathbf{k}} = \sum_{l=1}^N \left(k_l + \frac{1}{2} \right) \varphi_{\mathbf{k}}, \quad (4)$$

where $(q_l\psi)(x) = x_l\psi(x)$ and $(p_l\psi)(x) = -i\frac{\partial}{\partial x_l}\psi(x)$.

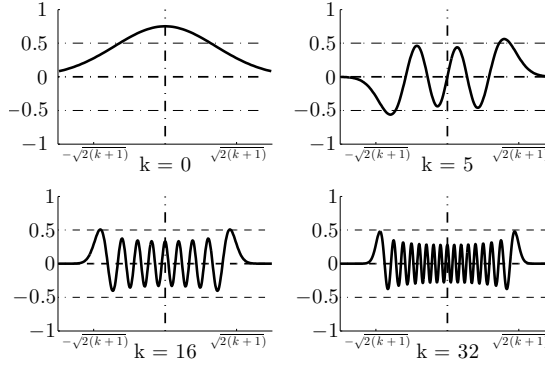


Figure 1: Univariate Hermite functions for some choices of k . φ_k is even if k is even, otherwise odd. The largest extremal is bounded by $\sqrt{2(k+1)}$.

1.2 Galerkin ansatz with reduced index set

An approximation

$$\psi_{\mathcal{K}}(x, t) = \sum_{\mathbf{k} \in \mathcal{K}} c_{\mathbf{k}}(t) \varphi_{\mathbf{k}}(x) \in \text{span} \{ \varphi_{\mathbf{k}} \mid \mathbf{k} \in \mathcal{K} \} \subseteq L^2(\mathbb{R}^N) \quad (5)$$

on a finite-dimensional subspace is determined such that

$$\left(i \frac{\partial}{\partial t} \psi_{\mathcal{K}} - H \psi_{\mathcal{K}}, \varphi_{\mathbf{j}} \right) = 0, \quad \forall \mathbf{j} \in \mathcal{K}, \quad (6)$$

where \mathcal{K} is a multi-dimensional index set

$$\mathcal{K} \subseteq \mathcal{K}_{\text{full}} = \{ \mathbf{k} = (k_1, \dots, k_N) \in \mathbb{N}^N \mid 0 \leq k_l \leq K \} \quad (7)$$

with at most $K + 1$ indices in each direction. If necessary, we write $\mathcal{K} = \mathcal{K}(K)$ to emphasize the bound K for components k_l of any $\mathbf{k} \in \mathcal{K}$. Abbreviating $c(t) = (c_{\mathbf{k}}(t))_{\mathbf{k} \in \mathcal{K}}$ and inserting the ansatz (5) into (6) yields a linear system of ODEs

$$i \dot{c}(t) = \mathcal{H}_{\mathcal{K}}(t) c(t).$$

Furthermore, the eigenfunction relation (4) yields a decomposition ($\mathbf{j}, \mathbf{k} \in \mathcal{K}$)

$$\begin{aligned} (\mathcal{H}_{\mathcal{K}})_{\mathbf{j}\mathbf{k}} &= (\varphi_{\mathbf{j}}, H \varphi_{\mathbf{k}}) = \left(\varphi_{\mathbf{j}}, \frac{1}{2} \left(-\Delta + \sum_{l=1}^N q_l^2 \right) \varphi_{\mathbf{k}} \right) + \left(\varphi_{\mathbf{j}}, \left(V - \frac{1}{2} \sum_{l=1}^N q_l^2 \right) \varphi_{\mathbf{k}} \right) \\ &= \sum_{l=1}^N \left(k_l + \frac{1}{2} \right) \delta_{\mathbf{j}\mathbf{k}} + (\varphi_{\mathbf{j}}, W \varphi_{\mathbf{k}}) = (\mathcal{D}_{\mathcal{K}})_{\mathbf{j}\mathbf{k}} + (\mathcal{W}_{\mathcal{K}})_{\mathbf{j}\mathbf{k}}, \end{aligned}$$

where $\mathcal{D}_{\mathcal{K}} = \text{diag}_{\mathbf{k} \in \mathcal{K}} \left(\sum_{l=1}^N (k_l + \frac{1}{2}) \right)$ is a diagonal matrix and $(\mathcal{W}_{\mathcal{K}})_{\mathbf{j}\mathbf{k}} = (\varphi_{\mathbf{j}}, W \varphi_{\mathbf{k}})$ stems from a multiplicative potential $W(x, t) = V(x, t) - \frac{1}{2} \sum_{l=1}^N x_l^2$. Hence,

$$i \dot{c}(t) = \mathcal{D}_{\mathcal{K}} c(t) + \mathcal{W}_{\mathcal{K}}(t) c(t). \quad (8)$$

In case $\mathcal{K} = \mathcal{K}_{\text{full}}$, the system (8) consists of $|\mathcal{K}| = (K + 1)^N$ equations. For growing N and K being only moderate, this is not feasible for time integration that requires assembling the matrices $\mathcal{D}_{\mathcal{K}}$ (once) and $\mathcal{W}_{\mathcal{K}}(t)$ (in each step) and multiplying them with a vector. Thus, the index set needs to be reduced. We study a hyperbolically reduced index set

$$\mathcal{K} = \left\{ \mathbf{k} = (k_1, \dots, k_N) \mid k_l \geq 0, \prod_{l=1}^N (1 + k_l) \leq K + 1 \right\},$$

see the illustration in Figure 2. The number of indices employed shrinks to $|\mathcal{K}| = \mathcal{O}(K \ln(K)^{N-1})$, see [8]. Approximating a sufficiently regular function by a Hermite tensor-product expansion over a hyperbolically reduced index set still gives a decent approximation, see [19], Thm. III.1.5.

Assumption on ψ : For any t , we assume the exact solution $\psi(\cdot, t)$ to be essentially supported within a cube $\Omega = [-L, L]^N$, for given K -independent L , possibly in a much smaller subregion (as in the case of a moving wavepacket). To vary resolution, we may define adequately compressed or stretched basis functions

$$\tilde{\varphi}_{\mathbf{k}}(x) = \prod_{l=1}^N \varphi_{k_l}(Sx_l), \quad \mathbf{k} \in \mathcal{K},$$

for some positive S . As the univariate φ_K is negligibly small outside the interval $[-\sqrt{2(K+1)} - 1, \sqrt{2(K+1)} + 1]$, we require S and K to be chosen such that

$$SL \geq \sqrt{2(K+1)} + 1.$$

For ease of presentation, we restrict ourselves to $S = 1$.

1.3 Approximation of the potential

Assumption on W : A basic assumption for our fast algorithm is that the potential W can be sufficiently well approximated by an interpolation polynomial W^{pol} on the cube $\Omega = [-L, L]^N$ indexed over a set $\mathcal{R}(R) \subseteq \mathbb{N}^N$ with only few nodes, i.e.,

$$|\mathcal{R}| \ll |\mathcal{K}|.$$

We consider Chebyshev interpolation on Ω over \mathcal{R} , i.e.,

$$W(x, t) \approx W^{\text{pol}}(x, t) = \sum_{\mathbf{r} \in \mathcal{R}} \alpha_{\mathbf{r}}(t) T_{\mathbf{r}}(x/L) = \sum_{\mathbf{r} \in \mathcal{R}} \alpha_{\mathbf{r}}(t) \prod_{l=1}^N T_{r_l}(x_l/L)$$

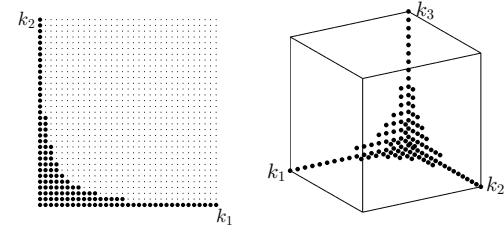


Figure 2: Hyperbolically reduced index set for $N = 2$ and $K = 32$ (left) and for $N = 3$ and $K = 16$ (right).

with coefficients $\alpha_{\mathbf{r}}(t)$. The univariate functions T_{r_i} are the Chebyshev polynomials of the first kind that obey the recurrence relation

$$\begin{aligned} T_0(x) &= 1, & T_1(x) &= x, \\ T_{k+1}(x) &= 2xT_k(x) - T_{k-1}(x), & k &\geq 1, \end{aligned} \quad x \in [-1, 1]. \quad (9)$$

In case of a full product grid $\mathcal{R} = \mathcal{R}_{\text{full}}$, we have exponentially decaying coefficients $\alpha_{\mathbf{r}}$, see, e.g., [9] for a detailed theory of approximation by orthogonal polynomials. In case of a reduced index set \mathcal{R} , a fast polynomial transform on sparse grids can be employed to compute the interpolation coefficients efficiently, see, e.g., [10] for an $\mathcal{O}(R \ln(R)^{N+1})$ algorithm with still exponentially decaying coefficients $\alpha_{\mathbf{r}}(t)$ (for W being sufficiently regular) with a hyperbolically reduced set \mathcal{R} . Due to $R \ll K$, the additional costs of doing polynomial interpolation in each time step are negligible. In place of (8), this yields a coefficient ODE

$$i\dot{c}_{\text{pol}}(t) = \mathcal{D}_{\mathcal{K}}c_{\text{pol}}(t) + \mathcal{W}_{\mathcal{K},\text{pol}}(t)c_{\text{pol}}(t). \quad (10)$$

2 Discretization in time

2.1 Need for matrix-vector products

The resulting coefficient initial value problem (10) is of the general form $i\dot{y}(t) = A(t)y(t)$ with a time-dependent Hermitian matrix $A(t)$ and initial value $y(0) = y_0$. Polynomial integrators of the form $y^{n+1} = P(-ihA(t))y^n$ as well as discretizations of the matrix exponential with a splitting procedure or a Magnus integrator each require multiplications of A with a vector in each time step. In the present paper, we restrict our attention to the latter choice, see [7], in particular, Sections 5 and 6, for numerical integration methods based on Magnus expansions. Magnus integrators consist of an exponential stepping procedure of the form $y^{n+1} = \exp(\Omega^n)y^n$, where $y^n \approx y(t_n)$, $t_n = hn$ with time-step size h , for a suitable choice of Ω^n . Possible choices are the exponential mid-point rule

$$\Omega^n = -ihA(t^n + h/2) \quad (11)$$

or the 2-stage Gauss-Legendre based method with nodes $c_{1,2} = \frac{1}{2} \mp \frac{\sqrt{3}}{6}$,

$$\Omega^n = -\frac{i}{2}h(A_1 + A_2) - \frac{\sqrt{3}}{12}h^2[A_2, A_1], \quad A_j = A(t^n + c_jh), \quad j = 1, 2, \quad (12)$$

where $[\cdot, \cdot]$ denotes the commutator of matrices. In our setting, we have

$$A(t) = \mathcal{H}_{\mathcal{K},\text{pol}}(t) = \mathcal{D}_{\mathcal{K}} + \mathcal{W}_{\mathcal{K},\text{pol}}(t).$$

[17] show that the methods (11) and (12) are of optimal temporal orders 2 and 4, respectively, for the Schrödinger equation with a bounded potential.

2.2 Lanczos method for the matrix exponential

We apply the Lanczos method in order to approximate the matrix exponential $\exp(\Omega^n)$, see [19], Chapter III.2.2, for a more detailed outline including further references and an algorithmic description. Consider a general initial value problem $i\dot{y}(t) = Ay(t)$ with an $d \times d$ Hermitian matrix A and $y(0) = y_0$. The Hermitian Lanczos process generates recursively the basis $V_m = (v_1 | \dots | v_m) \in \mathbb{C}^{d \times m}$ and a tridiagonal coefficient matrix $T_m \in \mathbb{C}^{m \times m}$ such that

$$T_m = V_m^* A V_m. \quad (13)$$

This requires m multiplications of A on a vector, where $m \ll d$. The matrices V_m and T_m are used to approximate

$$y(t) = \exp(-itA)y_0 \approx V_m \exp(-itT_m)e_1.$$

In our setting, we have $-ihA = \Omega^n$, $y_0 = y^n$. In each time step, for all specific choices of Ω^n , this involves the action of $\mathcal{W}_{\mathcal{K},\text{pol}}(t)$ on Lanczos vectors v_k , evaluated at times t depending on the chosen Magnus integrator.

3 The fast algorithm

3.1 Coordinate matrices for a direct operation

We consider the product of $\mathcal{W}_{\mathcal{K},\text{pol}}$, see (10), times an arbitrary vector $v \in \mathbb{C}^{|\mathcal{K}|}$. For each direction, we define coordinate matrices over an arbitrary index set \mathcal{K} by

$$X_{\mathcal{K}}^{(l)}, \quad 1 \leq l \leq N, \quad \left(X_{\mathcal{K}}^{(l)} \right)_{\mathbf{j}\mathbf{k}} = (\varphi_{\mathbf{j}}, q_l \varphi_{\mathbf{k}}), \quad \mathbf{j}, \mathbf{k} \in \mathcal{K}.$$

Due to the orthonormality of the basis and with the help of the one-dimensional recurrence relation (2), the action of $X_{\mathcal{K}}^{(l)}$ on v is given by

$$\begin{aligned} \left(X_{\mathcal{K}}^{(l)} v \right)_{\mathbf{j}} &= \sum_{\mathbf{k} \in \mathcal{K}} (\varphi_{\mathbf{j}}, q_l \varphi_{\mathbf{k}}) v_{\mathbf{k}} \\ &= \sum_{\mathbf{k} \in \mathcal{K}} \left(\varphi_{\mathbf{j}}, \sqrt{\frac{k_l + 1}{2}} \varphi_{\mathbf{k} + \mathbf{e}_l} + \sqrt{\frac{k_l}{2}} \varphi_{\mathbf{k} - \mathbf{e}_l} \right) v_{\mathbf{k}} = \sqrt{\frac{j_l}{2}} v_{\mathbf{j} - \mathbf{e}_l} + \sqrt{\frac{j_l + 1}{2}} v_{\mathbf{j} + \mathbf{e}_l}, \end{aligned} \quad (14)$$

for all $\mathbf{j} \in \mathcal{K}$ and $1 \leq l \leq N$. In case $j_l = 0$ or $j_l = k$, the next-to-last or last term vanishes, respectively. The matrix-vector-product $X_{\mathcal{K}}^{(l)} v$ can thus be computed directly using $\mathcal{O}(|\mathcal{K}|)$ operations.

3.2 Insertion into the polynomial

In case $W^{\text{pol}}(x) = x_l$, for some l , the Galerkin matrix reduces to the l -th coordinate matrix and $\mathcal{W}_{\mathcal{K},\text{pol}} v = X_{\mathcal{K}}^{(l)} v$. As proposed in [12], the idea is to compute $\mathcal{W}_{\mathcal{K},\text{pol}} v$ for

any polynomial W^{pol} by formally inserting the coordinate matrices into the polynomial. We can thus approximately compute

$$\begin{aligned} \mathcal{W}_{\mathcal{K},\text{pol}}(t)v &\approx W^{\text{pol}}(X_{\mathcal{K}},t)v = \sum_{\mathbf{r} \in \mathcal{R}} \alpha_{\mathbf{r}}(t) \left(\prod_{l=1}^N T_{r_l} \left(\frac{1}{L} X_{\mathcal{K}}^{(l)} \right) \right) v \\ &= \sum_{\mathbf{r} \in \mathcal{R}} \alpha_{\mathbf{r}}(t) \left(T_{r_1} \left(\frac{1}{L} X_{\mathcal{K}}^{(1)} \right) \cdot \left(\dots \left(T_{r_N} \left(\frac{1}{L} X_{\mathcal{K}}^{(N)} \right) v \right) \dots \right), \end{aligned} \quad (15)$$

where the products of $T_{r_l} \left(\frac{1}{L} X_{\mathcal{K}}^{(l)} \right)$ times a vector are computed with the help of the recurrence (9) using the direct operation (14).

3.3 Algorithmic description

The procedures as given in Figure 3 describe the fast algorithm for the action of $\mathcal{W}_{\mathcal{K},\text{pol}}(t)$ on a vector $v \in \mathbb{C}^{|\mathcal{K}|}$ for given index sets $\mathcal{K}(K)$ for the Galerkin basis and $\mathcal{R}(R)$ for the polynomial approximation $W^{\text{pol}}(x,t)$ of the potential over a cube (K -independent) $\Omega = [-L, L]^N$ with coefficients $\alpha_{\mathbf{r}}(t)$.

Given a time-step size h , a number m of Lanczos steps in each time step, and an initial

fast_algorithm	direct_operation
input: $\mathcal{K}(K), \mathcal{R}(R) \subset \mathbb{N}^N, (\alpha_{\mathbf{r}}(t))_{\mathbf{r} \in \mathcal{R}},$ $L \in \mathbb{R}, v \in \mathbb{C}^{ \mathcal{K} }$	input: $\mathcal{K}(K) \subset \mathbb{N}^N,$ $l \in \{1, \dots, N\}, v \in \mathbb{C}^{ \mathcal{K} }$
output: $\text{res} = W^{\text{pol}}(X_{\mathcal{K}}, t)v$	output: $\text{res} = X_{\mathcal{K}}^{(l)}v$
for $\mathbf{r} \in \mathcal{R}$ for $l = 1 : N$ $w_- = v$ $w_+ = \frac{1}{L} \text{direct_operation}(\mathcal{K}, l, v)$ for $r = 2 : r_l$ temp = w_+ $w_+ = \frac{2}{L} \text{direct_operation}(\mathcal{K}, l, w_+)$ $w_+ = w_+ - w_-, w_- = \text{temp}$ endfor $v = w_+$ endfor res = $\alpha_{\mathbf{r}}(t)v$ endfor	for $\mathbf{j} \in \mathcal{K}$ $\text{res}_{\mathbf{j}} = \begin{cases} \sqrt{\frac{1}{2}} v_{\mathbf{j}+\mathbf{e}_l}, & j_l = 0, \\ \sqrt{\frac{K}{2}} v_{\mathbf{j}-\mathbf{e}_l}, & j_l = K, \\ \sqrt{\frac{j_l}{2}} v_{\mathbf{j}-\mathbf{e}_l} + \sqrt{\frac{j_l+1}{2}} v_{\mathbf{j}+\mathbf{e}_l}, & \text{else.} \end{cases}$ endfor

Figure 3: Algorithmic description of the fast algorithm for a matrix-vector product using (9) and direct operation on a vector with $X_{\mathcal{K}}^{(l)}$.

coefficient vector c_{pol}^0 of unit norm, time propagation of (10) using a Magnus integrator is done as outlined in Figure 4. Step (1) has to be repeated in each time step in case of a time-dependent potential only. Step (3) is done using a (small) diagonalization of $T_m^{(n)}$, and the product $V_m^{(n)}$ times a vector is computed in $\mathcal{O}(|\mathcal{K}|m^2)$.

time_propagation	
input:	$\mathcal{K}(K), \mathcal{R}(R) \subset \mathbb{N}^N, h, L \in \mathbb{R}, m \in \mathbb{N}, c_{\text{pol}}^0 \in \mathbb{C}^{ \mathcal{K} }$
output:	$\text{res} = c_{\text{pol}}^{t_{\text{end}} h^{-1}} \approx c_{\text{pol}}(t_{\text{end}})$
for $n = 0, \dots, t_{\text{end}} h^{-1}$	
	(1) Compute coefficients $\alpha_{\mathbf{r}}(t)$ of $W^{\text{pol}}(x, t) = \sum_{\mathbf{r} \in \mathcal{R}} \alpha_{\mathbf{r}}(t) T_{\mathbf{r}}(x/L)$ as prescribed by the chosen integrator.
	(2) Do m Lanczos steps to obtain $V_m^{(n)} = (v_1 \dots v_m)$ and $T_m^{(n)}$ starting from $v_1 = c_{\text{pol}}^n$. In each Lanczos step, use: $(\mathcal{D}_{\mathcal{K}} v_k)_j = \sum_{l=1}^N (j_l + \frac{1}{2})(v_k)_j$ $W^{\text{pol}}(X_{\mathcal{K}}, t) v_k = \text{fast_algorithm}(\mathcal{K}, \mathcal{R}, (\alpha_{\mathbf{r}})_{\mathbf{r} \in \mathcal{R}}, L, v_k)$
	(3) Compute $c_{\text{pol}}^{n+1} = V_m^{(n)} \exp(-ihT_m^{(n)}) e_1$.
endfor	

Figure 4: Time propagation using the fast algorithm with a Magnus integrator.

3.4 Computational complexity.

For fixed l , `direct_operation` requires $\mathcal{O}(|\mathcal{K}|)$ operations. Thus, using (9), $T_{r_l} \left(\frac{1}{L} X_{\mathcal{K}}^{(l)} \right) v$ is computed in $\mathcal{O}(|\mathcal{K}| \cdot r_l)$ operations, which gives $\prod_{l=1}^N T_{r_l} \left(\frac{1}{L} X_{\mathcal{K}}^{(l)} \right) v$ in $\mathcal{O}(|\mathcal{K}| \cdot R \cdot N)$. Therefore, `fast_algorithm` allows to compute the product $W^{\text{pol}}(X_{\mathcal{K}}, t)v$ in

$$\mathcal{O}(|\mathcal{K}| \cdot |\mathcal{R}| \cdot R \cdot N)$$

operations. Because of $|\mathcal{R}| \ll |\mathcal{K}|$, in case of W being time-dependent, the costs for re-computing the coefficients of the interpolation polynomial in each step are negligible. In Figure 5, we consider a hyperbolically reduced index set \mathcal{K} and compare assembling $\mathcal{W}_{\mathcal{K}, \text{pol}}$ to a direct computation of $W^{\text{pol}}(X_{\mathcal{K}})v$ with respect to CPU time for a stretched torsional potential

$$W(x) = \sum_{l=1}^N (1 - \cos(x_l/L)), \quad x \in \Omega, \quad L = 16, \quad (16)$$

as approximated by Chebyshev interpolation over a hyperbolically reduced index set \mathcal{R} with $R = 8$ (yielding an interpolation error of size $\approx 1e-10$) giving computation times for some choices of N and K . The entries of $\mathcal{W}_{\mathcal{K}, \text{pol}}$ are discretized using Gauss-Hermite quadrature. As the figures reveal, on a hyperbolically reduced index set, the fast algorithm lowers the computational effort by several orders of magnitude for reasonable choices of K . The larger K , the better the reduction (for fixed N). All figures have been obtained with a FORTRAN 95 implementation on an Intel Core 2 Duo E8400 3.00 GHz processor with 4 GB RAM in double precision arithmetics.

N	K	(1)	(2)	$\approx (1)/(2)$
2	20	$1.475e-01$	$5.250e-04$	$2.8e+02$
	60	≈ 6 secs	$1.849e-03$	$3.3e+03$
	100	≈ 35 secs	$3.382e-03$	$1.0e+04$
3	20	$2.230e+00$	$2.691e-03$	$8.3e+02$
	60	> 2 min	$1.140e-02$	$1.2e+04$
	100	> 15 min	$2.326e-02$	$4.0e+04$
4	60	≈ 26 min	$5.170e-02$	$3.0e+04$

Figure 5: CPU times in secs for assembling the hyperbolically indexed matrix $\mathcal{W}_{\mathcal{K},\text{pol}}$ and multiplying it with a random vector $v \in \mathbb{R}^{|\mathcal{K}|}$ (column (1)) and for the fast algorithm (column (2)) with a torsional potential as given in (16) approximated by Chebyshev interpolation over hyperbolically reduced \mathcal{R} with $R = 8$. Last column: ratios of computation times.

4 Relation to Gauss-Hermite quadrature

4.1 Product Gauss-Hermite quadrature

In preparation for the subsequent error analysis, we consider Gaussian quadrature for the weight function e^{-x^2} over \mathbb{R} in each direction. Let ξ_m denote the zeros of H_{M+1} with corresponding weights w_m (see, e.g., [1], Section 25). The resulting quadrature formula $(w_m, \xi_m)_{m=0}^M$ is exact for polynomials of degree $\leq 2M + 1$. In higher dimensions, we set

$$\xi_{\mathbf{m}} = (\xi_{m_1}, \dots, \xi_{m_N}), \quad \omega_{\mathbf{m}} = \prod_{l=1}^N \omega_{m_l} = \prod_{l=1}^N w_{m_l} e^{\xi_{m_l}^2}, \quad \mathbf{m} \in \mathcal{M}_{\text{full}}(M),$$

with a full N -dimensional index set $\mathcal{M}_{\text{full}}(M)$. This yields a product quadrature

$$(\mathcal{W}_{\mathcal{K},\text{pol}}(t))_{\mathbf{j}\mathbf{k}} \approx (\mathcal{W}_{\mathcal{K},\text{pol}}^{\text{GH}(M)}(t))_{\mathbf{j}\mathbf{k}} = \sum_{\mathbf{m} \in \mathcal{M}} \omega_{\mathbf{m}} \varphi_{\mathbf{j}}(\xi_{\mathbf{m}}) W^{\text{pol}}(\xi_{\mathbf{m}}, t) \varphi_{\mathbf{k}}(\xi_{\mathbf{m}}),$$

which is exact if $W^{\text{pol}}(\cdot, t) H_{\mathbf{j}} H_{\mathbf{k}}$ is a polynomial of degree $\leq 2M + 1$ in each direction, where $H_{\mathbf{k}}(x) = \prod_{l=1}^N H_{k_l}(x_l)$ is a product of univariate Hermite polynomials. Using (2) and (9), it is readily seen that assembling $\mathcal{W}_{\mathcal{K},\text{pol}}^{\text{GH}(M)}$ requires $\mathcal{O}(|\mathcal{K}|^2 \cdot |\mathcal{R}| \cdot M \cdot N)$ operations.

For a practical matrix assembly, [19], Chapter III.1.2., discusses Smolyak quadrature on sparse grids (see [21, 24, 14]) adapted to the increasingly oscillatory behavior of the high-order Hermite functions and points out that a sufficiently accurate sparse grid quadrature requires not less than $\mathcal{O}(K^2 M)$ evaluations of the potential.

4.2 Insertion of coordinate matrices revisited

We define $X_{\text{full}}^{(l)} = X_{\mathcal{K}_{\text{full}}}^{(l)}$ to be the coordinate matrices over the full index set. The matrices

$$\Xi^{(l)} = \text{diag}_{\mathbf{k} \in \mathcal{K}}(\xi_{k_l}) \in \mathbb{R}^{|\mathcal{K}_{\text{full}}| \times |\mathcal{K}_{\text{full}}|}, \quad U_{\mathbf{j}\mathbf{k}} = \sqrt{\omega_{\mathbf{j}}} \varphi_{\mathbf{k}}(\xi_{\mathbf{j}}), \quad \mathbf{j}, \mathbf{k} \in \mathcal{K}_{\text{full}},$$

yield a diagonalization $X_{\text{full}}^{(l)} = U^T \Xi^{(l)} U \in \mathbb{R}^{|\mathcal{K}_{\text{full}}| \times |\mathcal{K}_{\text{full}}|}$, which is readily seen from

$$(U^T \Xi^{(l)} U)_{\mathbf{j}\mathbf{k}} = \sum_{\mathbf{m} \in \mathcal{K}} \omega_{\mathbf{m}} \xi_{m_l} \varphi_{\mathbf{j}}(\xi_{\mathbf{m}}) \varphi_{\mathbf{k}}(\xi_{\mathbf{m}}) = (\varphi_{\mathbf{j}}, \varphi_{\mathbf{k}})^{\text{GH}(K)} = (X_{\text{full}}^{(l)})_{\mathbf{j}\mathbf{k}},$$

by the fact that there are exactly $K + 1$ quadrature nodes in each direction and that this yields an exact integration. The matrix U is unitary, which follows from orthonormality of the basis and

$$(U^T U)_{\mathbf{j}\mathbf{k}} = \sum_{\mathbf{m} \in \mathcal{K}} u_{\mathbf{m}\mathbf{j}} u_{\mathbf{m}\mathbf{k}} = \sum_{\mathbf{m} \in \mathcal{K}} \omega_{\mathbf{m}} \varphi_{\mathbf{j}}(\xi_{\mathbf{m}}) \varphi_{\mathbf{k}}(\xi_{\mathbf{m}}) = (\varphi_{\mathbf{j}}, \varphi_{\mathbf{k}})^{\text{GH}(K)} = (\varphi_{\mathbf{j}}, \varphi_{\mathbf{k}}) = \delta_{\mathbf{j}\mathbf{k}}.$$

This allows to compute

$$X_{\text{full}}^{\mathbf{r}} = \left(X_{\text{full}}^{(1)} \right)^{r_1} \cdots \left(X_{\text{full}}^{(N)} \right)^{r_N} = \prod_{l=1}^N (U^T \text{diag}(\xi_{m_l}^{r_l}) U) = U^T \text{diag}(\xi_{\mathbf{m}}^{\mathbf{r}}) U, \quad (17)$$

and we get the following

Lemma 1. *Choosing $\mathcal{M} = \mathcal{K}_{\text{full}}$ (i.e., $M = K$) for the full product quadrature and basis index sets, respectively, we get*

$$W^{\text{pol}}(X_{\text{full}}, t)_{\mathbf{j}\mathbf{k}} = (\mathcal{W}_{\mathcal{K}_{\text{full}}, \text{pol}}^{\text{GH}(K)}(t))_{\mathbf{j}\mathbf{k}}, \quad \mathbf{j}, \mathbf{k} \in \mathcal{K}_{\text{full}},$$

where $W^{\text{pol}}(X_{\text{full}}, t)$ denotes formal insertion of $X_{\text{full}}^{(l)}$ into W^{pol} according to (17). \square

This argument is common in the context of DVR techniques, see [18]. The ordering of the factors $\left(X_{\text{full}}^{(l)} \right)^{r_l}$ in $W^{\text{pol}}(X_{\text{full}}, t)$ is arbitrary.

Deriving the equivalence of full product quadrature and formal insertion requires a bijection $\mathcal{M} \leftrightarrow \mathcal{K}_{\text{full}}$. Simultaneously reducing \mathcal{M} and $\mathcal{K}_{\text{full}}$ invalidates the exactness of the Gauss-Hermite quadrature, reducing only $\mathcal{K}_{\text{full}}$ makes the above diagonalization argument no longer correct at all. For a reduced index set $\mathcal{K} \subsetneq \mathcal{K}_{\text{full}}$, an assertion analogous to Lemma 1 can therefore not be expected. In the fast algorithm, we employ the above reduced coordinate matrices $X_{\mathcal{K}}^{(l)}$. Hence, we expect the fast algorithm to induce errors due to quadrature and index set reduction, and a consideration of full product quadrature facilitates the error analysis.

5 Error analysis

5.1 Preliminaries

Definition of errors: Consider an arbitrary vector $v \in \mathbb{C}^{|\mathcal{K}|}$. We are interested in computing the product $\mathcal{W}_{\mathcal{K}, \text{pol}}(t)v$ with a matrix $\mathcal{W}_{\mathcal{K}, \text{pol}}$ as given in Section 1.3. The

fast algorithm as developed in Section 3 gives rise to an error due to quadrature and to an error due to index set reduction, the former being given by

$$E^{\text{quad}} = (E_{\mathbf{j},\mathbf{k}})_{\mathbf{j},\mathbf{k} \in \mathcal{K}}, \quad E_{\mathbf{j},\mathbf{k}} = (\mathcal{W}_{\mathcal{K},\text{pol}}(t))_{\mathbf{j}\mathbf{k}} - (\mathcal{W}_{\mathcal{K},\text{pol}}^{\text{GH}(K)}(t))_{\mathbf{j}\mathbf{k}}. \quad (18)$$

Formally inserting the reduced coordinate matrices into the polynomial yields an error

$$W^{\text{pol}}(X_{\mathcal{K}}, t)v - \mathcal{W}_{\mathcal{K},\text{pol}}^{\text{GH}(K)}(t)v = [W^{\text{pol}}(X_{\mathcal{K}}, t)v - \Omega(W^{\text{pol}}(X_{\text{full}}, t)v)] + \underbrace{\left[\left(\Omega(W^{\text{pol}}(X_{\text{full}}, t)) - \mathcal{W}_{\mathcal{K},\text{pol}}^{\text{GH}(K)}(t) \right) \right]}_{\star} v,$$

where the operator

$$\Omega : \mathbb{C}^{|\mathcal{K}_{\text{full}}| \times |\mathcal{K}_{\text{full}}|} \rightarrow \mathbb{C}^{|\mathcal{K}| \times |\mathcal{K}|}, \quad \Omega(A) = (A_{\mathbf{j}\mathbf{k}})_{\mathbf{j},\mathbf{k} \in \mathcal{K}} \quad (19)$$

cuts a fully indexed matrix to a reduced index set. The difference \star vanishes by virtue of Lemma 1. One easily verifies

$$\Omega(W^{\text{pol}}(X_{\text{full}}, t)v) = \Omega(W^{\text{pol}}(X_{\text{full}}, t)\Omega_+(v))$$

where the operator

$$\Omega_+ : \mathbb{C}^{|\mathcal{K}|} \rightarrow \mathbb{C}^{|\mathcal{K}_{\text{full}}|}, \quad (\Omega_+(v))_{\mathbf{j}} = \begin{cases} v_{\mathbf{j}}, & \mathbf{j} \in \mathcal{K}, \\ 0, & \mathbf{j} \notin \mathcal{K}, \end{cases}$$

blows up a vector with zeros at indices missing in \mathcal{K} , and Ω is defined as in (19) both for matrices and vectors. Hence, the error due to index set reduction is given by

$$E^{\text{red}}(v) = (E_{\mathbf{j}})_{\mathbf{j} \in \mathcal{K}}, \quad E_{\mathbf{j}} = (W^{\text{pol}}(X_{\mathcal{K}}, t)v)_{\mathbf{j}} - (W^{\text{pol}}(X_{\text{full}}, t)\Omega_+(v))_{\mathbf{j}}, \quad \mathbf{j} \in \mathcal{K}. \quad (20)$$

Assumption: For the following error analysis, we make the general decay assumption

$$v_{\mathbf{k}} = \mathcal{O}(\mathbf{k}^{-\beta}) = \mathcal{O}\left(\prod_{\substack{l=1, \\ k_l \neq 0}}^N k_l^{-\beta}\right), \quad \mathbf{k} \in \mathcal{K}, \quad (21)$$

for the vector coefficients of v , with some $\beta \in \mathbb{N}$. The larger the index, the faster the decay. Assumption (21) is used in Sections 5.2 and 5.3 to compensate large error components in matrix-vector-products. For $\mathbf{r} \in \mathbb{N}^N$, we define $r_{\max}(\mathbf{r}) = \max_{1 \leq l \leq N} r_l$.

5.2 Error E^{quad} due to quadrature

Theorem 1. *Let $W^{\text{pol}}(\cdot, t) \approx W(\cdot, t)$ be the Chebyshev interpolation polynomial of the potential W on $\Omega = [-L, L]^N$ over $\mathcal{R}(R)$ for fixed L . Let $\mathcal{K}(K)$ be a hyperbolically*

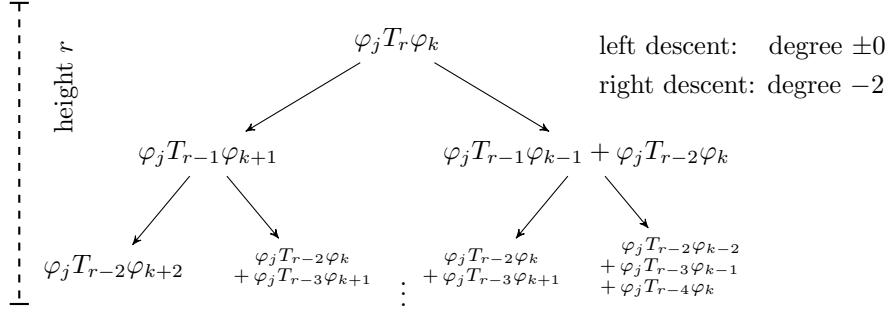


Figure 6: Expansion of 1D quadrature error as a binary tree. In case $r = 1$, we just use (2) on a term, in case $r = 0$, terms are added to the left child without expanding.

reduced index set with $K \gg R$. Then, under assumption (21) on $v \in \mathbb{C}^{|\mathcal{K}|}$ (i.e., componentwise decay of order $\beta \in \mathbb{N}$), the error due to quadrature behaves as

$$\left| \left(\left(\mathcal{W}_{\mathcal{K}, \text{pol}}(t) - \mathcal{W}_{\mathcal{K}, \text{pol}}^{\text{GH}(K)}(t) \right) v \right)_j \right| \leq C(\mathcal{R}, W, t) K^{-\beta}, \quad j \in \mathcal{K},$$

where the matrices $\mathcal{W}_{\mathcal{K}, \text{pol}}(t)$ and $\mathcal{W}_{\mathcal{K}, \text{pol}}^{\text{GH}(K)}(t)$ are defined according to Sections 1.3 and 4.1, respectively. The constant $C(\mathcal{R}, W, t)$ behaves as in (29), see below, and depends only on \mathcal{R} , the regularity of W , and time t .

Proof. Termwise consideration of W^{pol} gives rise to error matrices

$$E_{\mathbf{jk}}^{\text{quad}} = \sum_{\mathbf{r} \in \mathcal{R}} \alpha_{\mathbf{r}}(t) E_{\mathbf{jk}}^{\mathbf{r}}, \quad E_{\mathbf{jk}}^{\mathbf{r}} = (\varphi_{\mathbf{j}}(S \cdot), T_{\mathbf{r}}(\cdot/L) \varphi_{\mathbf{k}}(S \cdot)) - (\varphi_{\mathbf{j}}(S \cdot), T_{\mathbf{r}}(\cdot/L) \varphi_{\mathbf{k}}(S \cdot))^{\text{GH}(K)}.$$

Conversion of 1D-error into binary tree: In one dimension, applying recursions (9) and (2) yields a decomposition

$$\begin{aligned} \varphi_j(Sx) T_r(x/L) \varphi_k(Sx) &= \left(\frac{\sqrt{2(k+1)}}{SL} \varphi_j(Sx) T_{r-1}(x/L) \varphi_{k+1}(Sx) \right) \\ &+ \left(\frac{\sqrt{2k}}{SL} \varphi_j(Sx) T_{r-1}(x/L) \varphi_{k-1}(Sx) - \varphi_j(Sx) T_{r-2}(x/L) \varphi_k(Sx) \right). \end{aligned} \quad (22)$$

Due to $SL \geq \sqrt{2(K+1)} + 1$ (see Section 1.3), all coefficients are bounded by

$$\frac{\sqrt{2k}}{SL} \leq \frac{\sqrt{2(k+1)}}{SL} \leq 1. \quad (23)$$

Termwise r -fold application of (22) yields the binary tree pattern \mathfrak{T} as given in Figure 6 (arguments and coefficients omitted). Descending right reduces the polynomial degree by 2, descending left leaves it unaltered. In case $r > k$, we may define $\varphi_k(x) = 0$ for $k \leq -1$, preserving the recurrence relation (2) for negative indices. We expand

termwise until each leaf carries a single term of the form $\varphi_j \varphi_{k+\lambda-\rho}$, where ρ and λ are the numbers of index-changing right and left descents, respectively, $\lambda + \rho \leq r$. By the same procedure for the corresponding quadrature formulas, we convert E_{jk}^r into a binary tree \mathfrak{T} of height r . We examine non-vanishing leaves in \mathfrak{T} , how many these are, and what quantity they sum up to.

Characterization of non-vanishing leaves: Fix a leaf in \mathfrak{T} connected to the root E_{jk}^r by ρ and λ right and left descents, respectively. For the quadrature error not to vanish, we require $2(K+1) \leq j+k+\lambda-\rho$ for each single term. For the exact integral not to vanish, orthogonality yields the requirement $j = k + \lambda - \rho$, leading to the contradiction $2(K+1) \leq 2j$. Thus, leaves with non-vanishing quadrature errors carry only the quadrature formulas.

Number of non-vanishing leaves: The condition for a non-vanishing quadrature error at a particular leaf yields $2(K+1) \leq j+k+\lambda-\rho \leq j+k+r-2\rho$. We define

$$\rho_{\max}(j, k, r) = \left\lfloor \frac{j+k+r-2(K+1)}{2} \right\rfloor_+ \leq \frac{r}{2} - 1,$$

which is the maximal number of right descents that does not reduce the polynomial degree of the integrand sufficiently for exact quadrature, where $a_+ = a$ if $a \geq 0$, otherwise $a_+ = 0$. In an arbitrary full binary tree of height r , the number of leaves connected to the root by a path containing exactly s right descents equals $\binom{r}{s}$. Hence, the number of non-vanishing leaves in \mathfrak{T} is given by $a(j, k, r) := \sum_{s=0}^{\rho_{\max}} \binom{r}{s}$.

Consider the general sum $\sum_{s=a}^b \binom{c}{s}$ with $a, b, c \in \mathbb{N}$ and $a \leq 2b < c$. For $s \leq b$,

$$\binom{c}{s} / \binom{c}{b} = \frac{b!(c-b)!}{s!(c-s)!} = \frac{b \cdot \dots \cdot (s+1)}{(c-s) \cdot \dots \cdot (c-b+1)} < \left(\frac{b}{c-b+1} \right)^{b-s}.$$

The assumption $c > 2b$ implies $b/(c-b+1) < 1$. Therefore,

$$\sum_{s=a}^b \binom{c}{s} = \binom{c}{b} \sum_{s=a}^b \binom{c}{s} / \binom{c}{b} < \binom{c}{b} \sum_{s=a}^b \left(\frac{b}{c-b+1} \right)^{b-s} < \binom{c}{b} (b-a+1). \quad (24)$$

By definition, we have $2\rho_{\max} < r$, thus,

$$a(j, k, r) < \left(\left\lfloor \frac{r}{2} - 1 \right\rfloor_+ \right)^r. \quad (25)$$

At best, $j+k+r = 2K+2$, and we have $a(j, k, r) = 1$. At worst, $j, k = K$, thus, $\rho_{\max} = \left\lfloor \frac{r}{2} - 1 \right\rfloor_+$, which makes the last estimate almost sharp.

Error accumulation in 1D: Taking into account boundedness of the coefficients (23) and vanishing exact integrals at non-vanishing leaves, summing up yields

$$|E_{jk}^r| \leq a(j, k, r) \cdot \max_{\substack{0 \leq j \leq K, -r \leq k \leq K+r \\ j+k \geq 2K+2}} \left| \sum_{m=0}^K \omega_m \varphi_j(\xi_m) \varphi_k(\xi_m) \right| = a(j, k, r) \cdot \mu(K, r). \quad (26)$$

Due to cancellation effects by Hermite function evaluations with rapidly alternating signs, the term $\mu(K, r)$ is of size $\mathcal{O}(1)$.

Decomposition of error in multiple dimensions: We set $\mathcal{N} = \{1, \dots, N\}$ and consider the error matrix for $N \geq 2$. For arbitrary $\mathbf{j}, \mathbf{k} \in \mathcal{K}$ and $\mathbf{r} \in \mathcal{R}$: If $k_l \leq K - r_l + 1$, for all $l \in \mathcal{N}$, we have $j_l + k_l + r_l \leq 2K + 1$, and the one-dimensional error matrices $E_{j_l k_l}^{r_l}$ vanish, for all $l \in \mathcal{N}$. Hence, $E_{\mathbf{j}\mathbf{k}}^{\mathbf{r}} = 0$. Conversely, for fixed $\mathbf{j} \in \mathcal{K}$ and $\mathbf{r} \in \mathcal{R}$, if there is $\mathbf{k} \in \mathcal{K}$ such that $E_{\mathbf{j}\mathbf{k}}^{\mathbf{r}} \neq 0$, we find a subset of components $\tilde{\mathcal{N}} = \tilde{\mathcal{N}}(\mathbf{k}) \subseteq \mathcal{N}$ such that, for every $l \in \tilde{\mathcal{N}}$, $k_l \geq K - r_l + 2$, and $E_{j_l k_l}^{r_l}$ does not vanish. This allows for a decomposition (omitting factors M and L^{-1} in φ and T , respectively)

$$\begin{aligned} E_{\mathbf{j}\mathbf{k}}^{\mathbf{r}} &= (\varphi_{\mathbf{j}}, T_{\mathbf{r}} \varphi_{\mathbf{k}}) - (\varphi_{\mathbf{j}}, T_{\mathbf{r}} \varphi_{\mathbf{k}})^{\text{GH}(K)} = \left[\prod_{l=1}^N (\varphi_{j_l}, T_{r_l} \varphi_{k_l}) \right] - \left[\prod_{l=1}^N (\varphi_{j_l}, T_{r_l} \varphi_{k_l})^{\text{GH}(K)} \right] \\ &= \left\{ \underbrace{\left[\prod_{l \in \tilde{\mathcal{N}}} (\varphi_{j_l}, T_{r_l} \varphi_{k_l}) \right]}_{\mathbf{A}} - \underbrace{\left[\prod_{l \in \tilde{\mathcal{N}}} (\varphi_{j_l}, T_{r_l} \varphi_{k_l})^{\text{GH}(K)} \right]}_{\mathbf{B}} \right\} \underbrace{\left[\prod_{l \notin \tilde{\mathcal{N}}} (\varphi_{j_l}, T_{r_l} \varphi_{k_l}) \right]}_{\mathbf{C}} \end{aligned} \quad (27)$$

of a non-vanishing entry $E_{\mathbf{j}\mathbf{k}}^{\mathbf{r}}$. On a hyperbolically reduced set \mathcal{K} , non-vanishing errors $E_{\mathbf{j}\mathbf{k}}^{\mathbf{r}}$ have indices \mathbf{k} satisfying

$$K+1 \geq \prod_{l \in \mathcal{N}} (k_l + 1) = \left(\prod_{l \notin \tilde{\mathcal{N}}} (k_l + 1) \right) \left(\prod_{l \in \tilde{\mathcal{N}}} (k_l + 1) \right) \geq \left(\prod_{l \notin \tilde{\mathcal{N}}} (k_l + 1) \right) \left(\prod_{l \in \tilde{\mathcal{N}}} (K - r_l + 3) \right).$$

Clearly, for every $\mathbf{k} \in \mathcal{K}$, if $K \gg r_{\max}$, then $|\tilde{\mathcal{N}}(\mathbf{k})| \leq 1$. Thus, the terms \mathbf{A} and \mathbf{B} consist of exactly one factor each, and $\mathbf{A} - \mathbf{B}$ equals the one-dimensional quadrature error $E_{j_{l_0} k_{l_0}}^{r_{l_0}}$ for some $l_0 \in \mathcal{N}$.

Error estimation in multiple dimensions: Consider a non-vanishing entry $E_{\mathbf{j}\mathbf{k}}^{\mathbf{r}}$. By the above considerations for the one-dimensional case, the term \mathbf{A} vanishes. Due to $|\tilde{\mathcal{N}}(\mathbf{k})| = 1$, there is $l_0 \in \mathcal{N}$ such that \mathbf{B} equals $E_{j_{l_0} k_{l_0}}^{r_{l_0}}$. For a factor in \mathbf{C} , using Cauchy-Schwarz, we find $(\varphi_{j_l}, T_{r_l} \varphi_{k_l}) \leq C(r_l)$. Thus, from (25) and (26), we have

$$E_{\mathbf{j}\mathbf{k}}^{\mathbf{r}} = \mathcal{O} \left(E_{j_{l_0} k_{l_0}}^{r_{l_0}} \right) = \mathcal{O} \left(\left(\binom{r_{l_0}}{\lfloor \frac{r_{l_0}}{2} - 1 \rfloor_+} \right) \frac{r_{l_0}}{2} \right).$$

For a hyperbolically reduced index set $\mathcal{K}(K)$ with $R \leq \frac{K-1}{2} + 2$, it is easily seen that the total number of non-vanishing entries in $E^{\mathbf{r}}$ is at most $\frac{1}{2} r_{\max} (r_{\max} - 1)$. Multiplying the matrix with a rapidly decaying vector, we thus find

$$(E^{\mathbf{r}} v)_{\mathbf{j}} = \mathcal{O} \left(\frac{r_{\max}^2 (r_{\max} - 1)}{4} \left(\binom{r_{\max}}{\lfloor \frac{r_{\max}}{2} - 1 \rfloor_+} \right) (K - r_{\max} + 2)^{-\beta} \right). \quad (28)$$

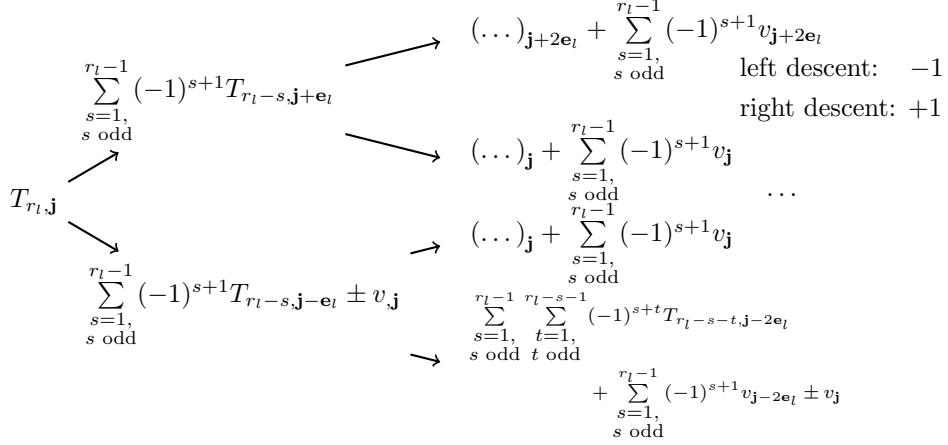


Figure 7: Expansion of $T_{r_l, \mathbf{j}}$ as a binary tree $\mathfrak{T}^{(l)}(\mathbf{j})$ of height r_l (90° rotation, coefficients omitted). The figure illustrates the case of r_l being even. Terms with reduced or unaltered index are attached to the left child, otherwise to the right child.

Summing up, the time-dependent and rapidly decaying interpolation coefficients enter into the constant

$$C(\mathcal{R}, W, t) = \sum_{\mathbf{r} \in \mathcal{R}} \alpha_{\mathbf{r}}(t) \frac{1}{4} r_{\max}^2 (r_{\max} - 1) \binom{r_{\max}}{\lfloor \frac{r_{\max}}{2} - 1 \rfloor_+}, \quad (29)$$

and, together with the assumption $K \gg R$, this proves the claim. \square

5.3 Error E^{red} due to index set reduction

Theorem 2. Let $W^{\text{pol}}(\cdot, t) \approx W(\cdot, t)$ be the Chebyshev interpolation polynomial of the potential W on $\Omega = [-L, L]^N$ over $\mathcal{R}(R)$ for fixed L . Let $\mathcal{K}(K)$ be a hyperbolically reduced index set with $K \gg R$. Then, under assumption (21) on $v \in \mathbb{C}^{|\mathcal{K}|}$ (i.e., componentwise decay of order $\beta \in \mathbb{N}$), the error due to index set reduction behaves as

$$\left| \left(\left(W^{\text{pol}}(X_{\mathcal{K}}, t) - \mathcal{W}_{\mathcal{K}, \text{pol}}^{\text{GH}(K)}(t) \right) v \right)_{\mathbf{j}} \right| \leq C(N, \mathcal{R}, W, \beta, L, t) K^{-\beta}, \quad \mathbf{j} \in \mathcal{K}.$$

The matrix $W^{\text{pol}}(X_{\mathcal{K}}, t)$ results from formally inserting the hyperbolically reduced coordinate matrices $X_{\mathcal{K}}^{(l)}$ into the polynomial (see Section 3) and $\mathcal{W}_{\mathcal{K}, \text{pol}}^{\text{GH}(K)}(t)$ is defined as in Section 4.1. The constant $C(N, \mathcal{R}, W, \beta, L, t)$ behaves as in (32), see below, and depends only on N, \mathcal{R} , the regularity of W , β, L , and time t .

Proof. As in the previous theorem, we consider a partition of the error

$$E^{\text{red}}(v)_{\mathbf{j}} = \sum_{\mathbf{r} \in \mathcal{R}} \alpha_{\mathbf{r}}(t) \left[\left(T_{\mathbf{r}} \left(\frac{1}{L} X_{\mathcal{K}} \right) v \right)_{\mathbf{j}} - \left(T_{\mathbf{r}} \left(\frac{1}{L} X_{\text{full}} \right) \Omega_+(v) \right)_{\mathbf{j}} \right], \quad \mathbf{j} \in \mathcal{K}.$$

Construction of binary trees: For fixed $l \in \{1, \dots, N\}$, $r_l \in \{1, \dots, R\}$ and $\mathbf{j} \in \mathcal{K}_{\text{full}}$, applying the Chebyshev recursion (9) together with (14) yields an expansion

$$T_{r_l, \mathbf{j}} = \frac{\sqrt{2j_l}}{L} \sum_{\substack{s=1, \\ s \text{ odd}}}^{r_l-1} (-1)^{s+1} T_{r_l-s, \mathbf{j}-\mathbf{e}_l} + \frac{\sqrt{2(j_l+1)}}{L} \sum_{\substack{s=1, \\ s \text{ odd}}}^{r_l-1} (-1)^{s+1} T_{r_l-s, \mathbf{j}+\mathbf{e}_l} + \tau_{r_l, \mathbf{j}},$$

where we use the abbreviations $T_{r_l, \mathbf{j}} = \left(T_{r_l} \left(\frac{1}{L} X_{\text{full}}^{(l)} \right) v \right)_{\mathbf{j}}$ and

$$\tau_{r_l, \mathbf{j}} = \begin{cases} \pm v_{\mathbf{j}}, & r_l \text{ even and } 4 \mid (\dagger) r_l, \\ \pm \frac{1}{L} \left(\sqrt{\frac{j_l}{2}} v_{\mathbf{j}-\mathbf{e}_l} + \sqrt{\frac{j_l+1}{2}} v_{\mathbf{j}+\mathbf{e}_l} \right), & r_l \text{ odd and } 4 \mid (\dagger) (r_l + 1). \end{cases}$$

Repeated application allows for a binary tree expansion $\mathfrak{T}^{(l)}(\mathbf{j})$ of height r_l as given in Figure 7 (coefficients omitted). With each left or right descent, all indices of newly expanded T -terms have their l -th component reduced or increased by 1, respectively. Clearly, leaves carry sums of at most $\frac{1}{2}r_l(r_l - 1)$ terms. Starting from $\mathbf{j} \in \mathcal{K}_{\text{full}}$, a binary tree $\mathfrak{T}_{\text{full}}(\mathbf{j})$ for the product

$$\left(T_{\mathbf{r}} \left(\frac{1}{L} X_{\text{full}} \right) v \right)_{\mathbf{j}} = \left(T_{r_1} \left(\frac{1}{L} X_{\text{full}}^{(1)} \right) \cdot \left(\dots \left(T_{r_N} \left(\frac{1}{L} X_{\text{full}}^{(N)} \right) v \right) \dots \right) \right)_{\mathbf{j}}$$

is then obtained by attaching to each term in each leaf of $\mathfrak{T}^{(l)}$ analogously defined trees $\mathfrak{T}^{(l+1)}$ starting from $l = 1$, such that a leaf in layer l is a root of a subtree in layer $l + 1$, see the pattern given in Figure 8, where the topmost and lowermost layers are numbered 1 and N , respectively. Along the path to a proper leaf in layer N (an N -leaf), let λ_l and ρ_l denote the number of left and right descents in layer l , respectively. Starting from \mathbf{j} , in layer l , only the l -th component of \mathbf{j} is changed.

The same considerations apply with $X_{\mathcal{K}}^{(l)}$ in place of $X_{\text{full}}^{(l)}$, yielding an analogously defined binary tree $\mathfrak{T}_{\mathcal{K}}(\mathbf{j})$ starting from $\mathbf{j} \in \mathcal{K}$. We consider the difference tree $\mathfrak{D}(\mathbf{j}) = \mathfrak{T}_{\mathcal{K}}(\mathbf{j}) - \mathfrak{T}_{\text{full}}(\mathbf{j})$ for $\mathbf{j} \in \mathcal{K}$, using the vectors $v \in \mathbb{C}^{|\mathcal{K}|}$ and $\Omega_+(v)$. If an index does not belong to $\mathcal{K}_{\text{full}}$ or \mathcal{K} , we say that the corresponding term *vanishes* in $\mathfrak{T}_{\text{full}}(\mathbf{j})$ or $\mathfrak{T}_{\mathcal{K}}(\mathbf{j})$, respectively. A term in the difference tree $\mathfrak{D}(\mathbf{j})$ *vanishes* if corresponding terms in $\mathfrak{T}_{\text{full}}(\mathbf{j})$ and $\mathfrak{T}_{\mathcal{K}}(\mathbf{j})$ vanish or do not vanish both at the same time. We state the following obvious, yet important observations: Terms with an index belonging not even to $\mathcal{K}_{\text{full}}$ vanish in $\mathfrak{D}(\mathbf{j})$ anyway. An N -leaf does not vanish in $\mathfrak{D}(\mathbf{j})$ iff, along the path connecting it to the root $v_{\mathbf{j}}$, there is at least one node belonging to $\mathcal{K}_{\text{full}} \setminus \mathcal{K}$. As in Section 5.2, we examine non-vanishing N -leaves in $\mathfrak{D}(\mathbf{j})$.

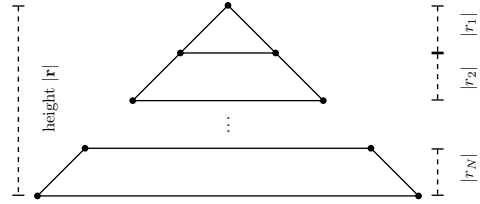


Figure 8: Layerwise attaching to form \mathfrak{T} .

Characterization of non-vanishing leaves: We consider a root index \mathbf{m} in layer l , where $m_l = j_l$. We have the following requirements for a term depending on \mathbf{m} not to vanish in $\mathfrak{T}_{\text{full}}(\mathbf{j})$ or $\mathfrak{T}_{\mathcal{K}}(\mathbf{j})$, respectively:

($\mathfrak{T}_{\text{full}}$) For the l -th component index, it is required $0 \stackrel{!}{\leq} j_l + \rho_l - \lambda_l \leq j_l + r_l - 2\lambda_l \stackrel{!}{\leq} K$, which gives the bounds

$$\lambda_{\min}^l(\mathbf{r}, \mathbf{j}) = \left\lfloor \frac{j_l + r_l - K}{2} \right\rfloor \leq \lambda_l \leq \left\lfloor \frac{j_l + r_l}{2} \right\rfloor = \lambda_{\max}^l(\mathbf{r}, \mathbf{j}).$$

($\mathfrak{T}_{\mathcal{K}}$) The upper bound is the same as in ($\mathfrak{T}_{\text{full}}$). By definition of \mathcal{K} , one needs

$$j_l + r_l - 2\lambda_l + 1 \stackrel{!}{\leq} (K + 1) \left(\prod_{\substack{i=1 \\ i \neq l}}^N (1 + m_i) \right)^{-1}. \quad (30)$$

From $\mathbf{m} \in \mathcal{K}$, it follows

$$1 + j_l \leq (K + 1) \left(\prod_{\substack{i=1 \\ i \neq l}}^N (1 + m_i) \right)^{-1},$$

thus, $r_l - 2\lambda_l \stackrel{!}{\leq} 0$ by subtraction, i.e., the leaf in $\mathfrak{T}_{\mathcal{K}}(\mathbf{j})$ does not vanish for

$$\lambda_l \geq \left\lceil \frac{r_l}{2} \right\rceil = \lambda_{\min, \text{hyp}}^l(\mathbf{r}). \quad (31)$$

Non-vanishing leaves in $\mathfrak{D}(\mathbf{j})$ satisfy ($\mathfrak{T}_{\text{full}}$), but not the more restrictive ($\mathfrak{T}_{\mathcal{K}}$). The converse is not true, since a leaf violating $\mathfrak{T}_{\mathcal{K}}$ might still fulfill condition (30), thus, vanish in $\mathfrak{D}(\mathbf{j})$. We consider the simpler condition (31). Obviously, $\lambda_{\min}^l \leq \lambda_{\min, \text{hyp}}^l$. *Number of non-vanishing leaves:* Summing up as in Section 5.2, we have at most

$$\sum_{s=\lambda_{\min}^l}^{\lambda_{\max}^l} \binom{r_l}{s} - \sum_{s=\lambda_{\min, \text{hyp}}^l}^{\lambda_{\max}^l} \binom{r_l}{s} = \sum_{s=\lambda_{\min}^l}^{\lambda_{\min, \text{hyp}}^l - 1} \binom{r_l}{s} = a_l(\mathbf{r}, \mathbf{j})$$

non-vanishing l -leaves. We use (24) with $a = \lambda_{\min}^l$, $b = \lambda_{\min, \text{hyp}}^l - 1$, $c = r_l$. The fact $\lambda_{\min, \text{hyp}}^l = \left\lceil \frac{r_l}{2} \right\rceil$ implies $2(\lambda_{\min, \text{hyp}}^l - 1) < r_l$, hence,

$$a_l(\mathbf{r}, \mathbf{j}) < \binom{r_l}{\lfloor \frac{r_l}{2} - 1 \rfloor} \frac{r_l}{2}.$$

Error accumulation: Along the path to any l -leaf, the most unfavorable weight

$$b_l(\mathbf{r}, \mathbf{j}) = 2^{r_l/2} \prod_{s=1}^{r_l} \frac{(j_l + s)^{1/2}}{L}$$

comes from descending right only. Using (21), the largest N -leaf is bounded by

$$c(\mathbf{r}, \mathbf{j}) \leq \prod_{l=1}^N \frac{1}{2} r_l (r_l - 1) \left\{ \max_{-r_l \leq s \leq r_l} |v_{\mathbf{j}-s\mathbf{e}_l}| \right\} = \mathcal{O} \left(\prod_{l=1}^N \frac{1}{2} r_l (r_l - 1) (j_l - r_l)^{-\beta} \right).$$

A path in $\mathfrak{D}(\mathbf{j})$ does not vanish only in case $\mathbf{j} + \mathbf{r} \in \mathcal{K}_{\text{full}} \setminus \mathcal{K}$, thus,

$$K+2 \leq \prod_{l=1}^N (1+j_l+r_l) = \prod_{l=1}^N (j_l-r_l) \cdot \prod_{l=1}^N \left(1 + \frac{1+2r_l}{j_l-r_l} \right) \leq \prod_{l=1}^N (j_l-r_l) \cdot 2^N \prod_{l=1}^N (1+r_l).$$

Hence, the error over all layers is bounded as

$$\begin{aligned} |E_{\mathbf{j}}^{\mathbf{r}}| &\leq \prod_{l=1}^N \{a_l(\mathbf{r}, \mathbf{j}) \cdot b_l(\mathbf{r}, \mathbf{j})\} \cdot c(\mathbf{r}, \mathbf{j}) \\ &= \mathcal{O} \left(2^{(\beta-2)N} \prod_{l=1}^N \left\{ \binom{r_l}{\lfloor \frac{r_l}{2} - 1 \rfloor} \cdot 2^{r_l/2} \prod_{s=1}^{r_l} \frac{(j_l+s)^{1/2}}{L} \cdot r_l^{\beta+3} (K+2)^{-\beta} \right\} \right) \end{aligned}$$

Finally, we sum up and set

$$C(N, \mathcal{R}, W, \beta, L, t) = \sum_{\mathbf{r} \in \mathcal{R}} \alpha_{\mathbf{r}}(t) 2^{(\beta-2)N} \prod_{l=1}^N \left\{ \binom{r_l}{\lfloor \frac{r_l}{2} - 1 \rfloor} \cdot 2^{r_l/2} \prod_{s=1}^{r_l} \frac{(j_l+s)^{1/2}}{L} \cdot r_l^{\beta+3} \right\} \quad (32)$$

Remarks: According to the choice of $\mathbf{j} \in \mathcal{K}$ or $\mathcal{R}(R)$, the above error estimate might improve. If there is more than one large component in \mathbf{j} , say $n(\mathcal{R}, \mathbf{j}) = \min_{\mathbf{r} \in \mathcal{R}} n(\mathbf{r}, \mathbf{j}) \geq 2$, where $n(\mathbf{r}, \mathbf{j}) \in \{1, \dots, N\}$ is the number of components j_l such that $K \approx j_l \gg r_l$, we get $c(\mathbf{r}, \mathbf{j}) = \mathcal{O}(K^{-n(\mathcal{R}, \mathbf{j})\beta})$. On the other hand, if $\mathbf{j} + \mathbf{r} \in \mathcal{K}$ (i.e., only small index components), all paths in $\mathfrak{D}(\mathbf{j})$ cancel out and the error $E_{\mathbf{j}}^{\mathbf{r}}$ vanishes altogether. \square

6 Numerical experiments

All figures have been obtained with a FORTRAN 95 implementation on an Intel Core 2 Duo E8400 3.00 GHz processor with 4 GB RAM in double precision arithmetics.

6.1 Local errors due to quadrature and index set reduction

Let $\mathcal{K} = \mathcal{K}(K)$ be a hyperbolically reduced N -dimensional index set. We illustrate the errors

$$E^{\text{quad}} v = \left(\mathcal{W}_{\mathcal{K}, \text{pol}} - \mathcal{W}_{\mathcal{K}, \text{pol}}^{\text{GH}(K)} \right) v, \quad E^{\text{red}}(v) = \left(W^{\text{pol}}(X_{\mathcal{K}}) - \mathcal{W}_{\mathcal{K}, \text{pol}}^{\text{GH}(K)} \right) v$$

due to quadrature and index set reduction as given in Theorems 1 and 2, respectively, for different choices of N and K , see Figure 9. In both cases, the chosen potential is a

stretched torsional potential as given in (16) approximated by Chebyshev interpolation over a hyperbolically reduced set. For the vector $v \in \mathbb{C}^{|\mathcal{K}|}$ to exhibit a decay behavior according to (21), we set $v_{\mathbf{k}} = \prod_{l=1}^N k_l^{-\beta}$, $\beta = 5$, and normalize such that $\|v\|_2 = 1$. As explained in Section 5.3, for K being sufficiently large, the error $(E^{\text{red}}(v))_{\mathbf{j}}$ decreases the faster the more components j_l of \mathbf{j} are large with respect to R , see Theorem 2 and the remarks thereafter. Figure 10 illustrates this decay behavior in the individual components of $E^{\text{red}}(v)$ for $N = 2$.

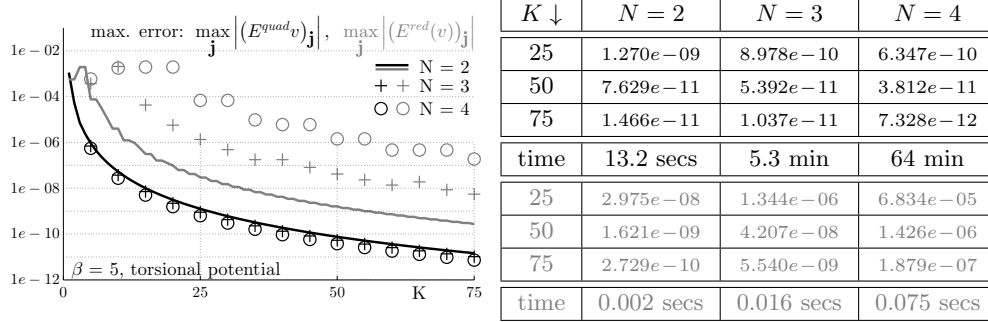


Figure 9: Errors $E^{\text{quad}}v$ (black) and $E^{\text{red}}(v)$ (gray) for the torsional potential (16) ($L = 16$, $S = 1$, reduced Chebyshev interpolation, $R = 8$, $\beta = 5$). The solid lines represent $N = 2$, selected errors in cases $N = 3, 4$ are indicated by plus signs and circles, respectively. Increasing N worsens the factor $C(N, \mathcal{R}, W, \beta, L)$ in E^{red} , see (32). In the rows labeled “time”, computation times for $\mathcal{W}_{\mathcal{K}, \text{pol}}^{\text{GH}(K)}v$ (assembly and multiplication) and for the fast algorithm in case $K = 75$ are shown. As for $N = 4$, assembling the matrix (plus operating on a vector) takes more than one hour – even on a reduced set.

6.2 Perturbed Lanczos process

We approximate the matrix exponential $\exp(-ih\mathcal{W}_{\mathcal{K}, \text{pol}})v$ using an m -step Lanczos process. Again, W is the above torsional potential ($L = 16$, $S = 1$, Chebyshev interpolation, $R = 8$) and v is given as above. In each Lanczos step for a problem of the form $i\dot{y}(t) = Ay(t)$, using the fast algorithm

$$(Av_k)^{\text{fast}} = Av_k - (Av_k - (Av_k)^{\text{fast}}) = Av_k - f_k$$

instead of Av_k produces perturbed basis vectors and coefficients \tilde{V}_m and \tilde{T}_m , respectively. This yields $A = \tilde{V}_m \tilde{T}_m \tilde{V}_m^* + F_m \tilde{V}_m^*$, where $F_m = (f_1 | \dots | f_m)$. Thus, by (13), $V_m T_m V_m^* = \tilde{V}_m \tilde{T}_m \tilde{V}_m^* + F_m \tilde{V}_m^*$. We approximate $\exp(-ihA)v \approx \tilde{V}_m \exp(-ih\tilde{T}_m)e_1$, and, by a sensitivity analysis for the matrix exponential as done in [23], the local error is readily seen to be

$$\left\| V_m \exp(-ihT_m)e_1 - \tilde{V}_m \exp(-ih\tilde{T}_m)e_1 \right\|_2 \leq h \|F_m\|_2 \exp(h(\|A\|_2 + \|F_m\|_2)). \quad (33)$$

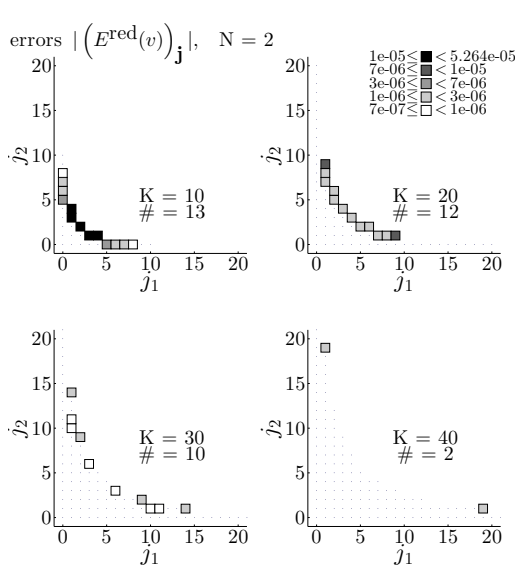


Figure 10: Errors $(E^{\text{red}}(v))_j$, due to index set reduction for a torsional potential with $N = 2$ and different choices of K (as above, $L = 16$, $S = 1$, $R = 8$, $\beta = 8$). Each entry represents an error vector component with an index from a hyperbolically reduced set. Errors being small with respect to the largest observed error component $e_{\max} \approx 5.264e-05$ are simply indicated by a dot, indices carrying larger errors are indicated by a grey box. The darker the box, the closer the error to e_{\max} . The pictures corresponding to $K = 30, 40$ show an enlarged view. The symbol $\#$ points to the number of large error components. Clearly, the errors decrease with growing K as indicated by increasingly lighter boxes and are concentrated in the region with only “intermediate” index components.

Here, $A = \mathcal{W}_{\mathcal{K}, \text{pol}}$. Hence, the error goes to zero if h is sufficiently small and the fast algorithm is sufficiently accurate. Note, however, that if m is chosen too large the vectors v_k , $k \geq 2$, might fail to decay sufficiently fast, and the perturbation error dominates the error due to Lanczos itself. Thus, we have to restrict ourselves to sufficiently small m (say, $m \approx 5$). See Figure 11 for some numerical results.

perturbation of Lanczos procedure				
$N = 2$, $K = 25$, $\beta = 3$, torsional potential				(33)
				classical
$m \downarrow$	$h \rightarrow$	1/10	1/20	1/40
2		$4.156e-07$	$2.079e-07$	$1.039e-07$
		$1.650e-03$	$4.128e-04$	$1.032e-04$
4		$4.296e-07$	$2.084e-07$	$1.040e-07$
		$2.011e-05$	$1.275e-06$	$8.000e-08$
6		$4.200e-07$	$2.080e-07$	$1.040e-07$
		$2.767e-07$	$4.520e-09$	$7.142e-11$

Figure 11: Error due to a perturbation of the Lanczos process by the fast algorithm (see (33), black figures) vs. error due to classical Lanczos without using the fast algorithm (gray figures) for $N = 2$ and $K = 25$ (as above, $L = 16$, $S = 1$, $R = 8$, $\beta = 3$). Clearly, increasing m or decreasing h improves the error due to Lanczos. However, if m is not sufficiently small, the error due to the perturbation becomes dominant.

6.3 Time integration

We consider two instances of the general equation (1). First, as a time-independent problem, consider once again the stretched torsional potential (16) (reduced Chebyshev interpolation, $R = 8$) for $N = 2$ and $K = 75$. The resulting ODE (10) is integrated over $[0, 1]$ with initial value c_{pol}^0 of decay order $\beta = 5$ using the (time-independent)

scheme (11) of order 2 for different choices of m and h , see Figure 12 (left). Second, as a time-dependent example, consider a stretched Hénon-Heiles potential with a linear time-dependent perturbation, i.e.,

$$V(x, t) = \sum_{l=1}^{N-1} \left[(x_l/L)^2(x_{l+1}/L) - \frac{1}{3}(x_{l+1}/L)^3 \right] - \sin^2(t)x_1, \quad x \in [-L, L]^N, \quad (34)$$

where $L = 16$ and $S = 1$ as above. This models the interaction of an atome / a molecule with a high-intensity CW laser in x_1 -direction, see [20] (with a quantum Harmonic oscillator in place of a HH-potential). We choose $N = 3$, $m = 5$, $\beta = 3$, and test with varying K . To represent the corresponding potential W , fully-indexed Chebyshev interpolation with $R = 3$ is used. Convergence results using the scheme (12) of order 4 are shown in Figure 12 (right).

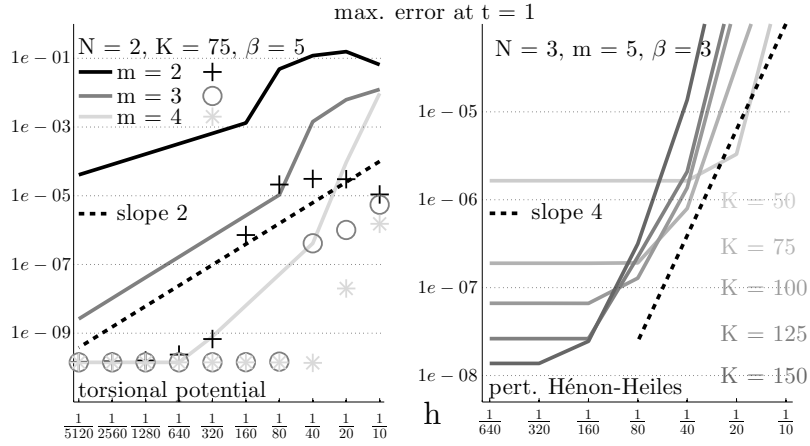


Figure 12: Left: Error $\max_j |c_{\text{pol}}^n - c_{\text{pol}}(t^n)|_{j \in \mathcal{K}}$ at time $t^n = 1$ when integrating (1) with $V(x)$ as in (16) ($N = 2$, $K = 75$, $L = 16$, $S = 1$, $R = 8$, $\beta = 5$) using the scheme (11) with different choices of time step h . The number m of Lanczos steps varies as indicated in the figure. Corresponding errors due to a perturbation of Lanczos are indicated by plus signs, circles, and asterisks, respectively. If m is too small ($m = 2$), the error due to Lanczos itself is dominant. The choice $m = 3$ makes visible the desired order of convergence until the perturbation error becomes dominant, whereas for $m = 4$, the latter error dominates even for moderate h . Right: Same with $V(x, t)$ as in (34) ($N = 3$, $m = 5$, $L = 16$, $S = 1$, $R = 3$, $\beta = 3$) using the scheme (12) with different choices of K . Clearly, the perturbation error dominates unless K is chosen sufficiently large. To obtain a reference, (12) has been employed with $h = 1e-5$ and 15 Lanczos steps in each time step.

Conclusion

We have presented a fast algorithm for the efficient treatment of the coefficient ODE resulting from spatial discretization of the linear Schrödinger equation in higher di-

mensions by a spectral Galerkin method. As time discretization of this ODE typically involves products of the time-dependent Galerkin matrix with a vector, assembling this matrix and doing the multiplication explicitly is prohibitive due to the complexity of the problem – even with a reduced basis and even more so in each time step. The fast algorithm provides a direct approach for this problem to circumvent complexity issues and reduce computational efforts considerably. It consists of a Horner-like, fast application of coordinate matrices formally inserted into the polynomially approximated potential. Using a full index set, this procedure is equivalent to Gauss-Hermite quadrature with exactly as many nodes as there are basis functions in each direction. For a hyperbolically reduced index set, we have analyzed the resulting quadrature and index set reduction errors by casting the problem as an examination on binary trees. As it turns out, if the underlying potential is sufficiently smoother than the exact solution, both errors decay rapidly. We point out that the fast algorithm constitutes a generic strategy that can be applied for spectral discretizations of linear problems based on orthogonal polynomials other than the Schrödinger equation with Hermite functions.

Acknowledgement: The author is grateful to Christian Lubich for his valuable suggestions and helpful discussions. Bernd Brumm is funded by the DFG Priority Program 1324 and is associated with DFG Research Training Group 1838.

References

- [1] M. Abramowitz and I.A. Stegun, *Handbook of Mathematical Functions*, Dover, New York, 1972 (10th printing).
- [2] G. Avila and T. Carrington, *Nonproduct quadrature grids for solving the vibrational Schrödinger equation*, *J. Chem. Phys.*, 131 (2009), doi: 10.1063/1.3246593.
- [3] ..., *Using nonproduct quadrature grids to solve the vibrational Schrödinger equation in 12D*, *J. Chem. Phys.*, 134 (2011), doi: 10.1063/1.3549817.
- [4] ..., *Using a pruned basis, a non-product quadrature grid, and the exact Watson normal-coordinate kinetic energy operator to solve the vibrational Schrodinger equation for C2H4*, *J. Chem. Phys.*, 135 (2011), doi: 10.1063/1.3617249.
- [5] ..., *Solving the vibrational Schrodinger equation using bases pruned to include strongly coupled functions and compatible quadratures*, *J. Chem. Phys.*, 137 (2012), doi: 10.1063/1.4764099.
- [6] ..., *Solving the Schroedinger equation using Smolyak interpolants*, *J. Chem. Phys.*, 139 (2013), doi: 10.1063/1.4821348.
- [7] S. Blanes, F. Casas, J.A. Oteo and J. Ros, *The Magnus expansion and some of its applications*, *Physics Reports*, 470 (2009), pp. 151–238.

- [8] H.-J. Bungartz and M. Griebel, *Sparse Grids*, Acta Numerica, 13 (2004), pp. 147–269.
- [9] C. Canuto, A. Quarteroni, M.Y. Hussaini, and T.A. Zang, *Spectral Methods: Fundamentals in Single Domains*, Springer, Berlin, 2006.
- [10] Y. Cao, Y. Jiang, and Y. Xu, *A fast algorithm for orthogonal polynomial expansions on sparse grids*, to appear in Journal of Complexity, retrieved from <http://www.auburn.edu/~yzc0009/publication/cao-jiang-xu8-30-13.pdf>.
- [11] E. Faou and V. Gradinaru, *Gauss-Hermite wavepacket dynamics: convergence of the spectral and pseudo-spectral approximation*, IMA J. Nume. Anal., 29 (2009), pp. 1023–1045.
- [12] E. Faou, V. Gradinaru, and Ch. Lubich, *Computing semiclassical quantum dynamics with Hagedorn wavepackets*, SIAM J. Sci. Comp., 31 (2009), pp. 3027–3041.
- [13] L. Gauckler, *Convergence of a split-step Hermite method for the Gross-Pitaevskii equation*, IMA J. Numer. Anal., 31 (2011), pp. 396–415.
- [14] T. Gerstner and M. Griebel, *Numerical integration using sparse grids*, Numer. Algor., 18 (1998), pp. 209–232.
- [15] V. Gradinaru, *Fourier Transform on Sparse Grids: Code Design and Application to the Time Dependent Schrödinger Equation*, Computing, 80 (2007), pp. 1–22.
- [16] ..., *Strang Splitting for the Time Dependent Schrödinger Equation on Sparse Grids*, SIAM J. Numer. Analysis, 46 (2007), pp. 103–123.
- [17] M. Hochbruck and Ch. Lubich, *On Magnus integrators for time-dependent Schrödinger equations*, SIAM J. Numer. Anal., 41 (2003), pp. 945–963.
- [18] J.C. Light and T. Carrington, *Discrete variable representations and their utilization*, Adv. Chem. Phys., 114 (2000), pp. 263–310.
- [19] Ch. Lubich, *From Quantum to Classical Molecular Dynamics: Reduced Models and Numerical Analysis*, Europ. Math. Soc., Zurich, 2008.
- [20] U. Peskin, R. Kosloff and N. Moiseyev, *The Solution of the Time-Dependent Schrödinger Equation by the (t, t') Method: The Use of Global Polynomial Propagators for Time-Dependent Hamiltonians*, J. Chem. Phys., 100 (1994), pp. 8849–8855.
- [21] S.A. Smolyak, *Quadrature and interpolation formulas for tensor products of certain classes of functions*, Dokl. Akad. Nauk SSSR, 4 (1963), pp. 240–243.
- [22] B. Thaller, *Visual Quantum Mechanics*, Springer, New York, 2000.
- [23] Ch. Van Loan, *The Sensitivity of the Matrix Exponential*, SIAM J. Numer. Anal., 14 (1977), 971–981.

- [24] Ch. Zenger, *Sparse Grids*, in: Parallel algorithms for partial differential equations, Notes on Numerical Fluid Mechanics 31, W. Hackbusch, ed., Vieweg, Braunschweig, 1991, pp. 241–251.